

To: Distribution
From: Ron Schulze
Subject: Performance of the New Horizon High Gain Antenna System

Introduction:

The purpose of this memorandum is to provide a brief description of the New Horizon Antenna system and to report on its measured performance. The New Horizon (NH) program is NASA's inaugural New Frontier's class interplanetary mission that will conduct the first reconnaissance of the Pluto-Charon system and a yet unidentified Kuiper Belt Object (KBO). The baseline launch date for the NH mission is January 2006 and the Pluto-Charon encounter will occur in early 2016. Prior to these encounters, there will be lengthy hibernation periods with no ground contact to minimize mission operations costs. The relevance to the antenna system is that the spacecraft will be spin stabilized at all times except during encounters to maintain a fixed spacecraft attitude and all of the antenna patterns are symmetrical about the spacecraft spin axis to allow routine and emergency operations while spinning

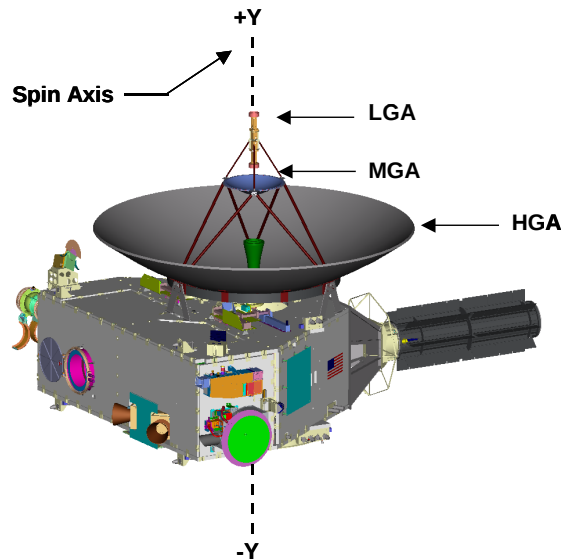


Figure 1: Forward Side of the New Horizon Observatory

This results in a stack arrangement of the antennas (HGA, medium gain antenna (MGA), and low gain antenna (LGA)) on the forward side of the New Horizon observatory as shown in Figure 1. This configuration is best because it satisfies the communication system requirements and stringent mass limitations imposed by the mission. The packaging of the antennas was initially selected based on the requirement that the

forward (+Y) low gain antenna be located on or near the spin axis and provide communications coverage, $\pm 90^\circ$ from the spin axis, which limits possible locations for the MGA and HGA. In order to satisfy the clear field of view requirement of $\pm 90^\circ$ for the +Y LGA, the only feasible location for 2.1-meter HGA is on the spin axis, as shown, with the LGA mounted above the HGA sub-reflector. Some consideration was given to relocating the MGA off the spin axis and near the rim of the HGA but was prohibitive in terms of additional mass, its field of view requirement, and excessive RF coupling from the HGA system. It was determined that the configuration shown in Figure 1 is the most efficient placement of the MGA system. The aft LGA is also on the spin axis, as shown in Figure 2.

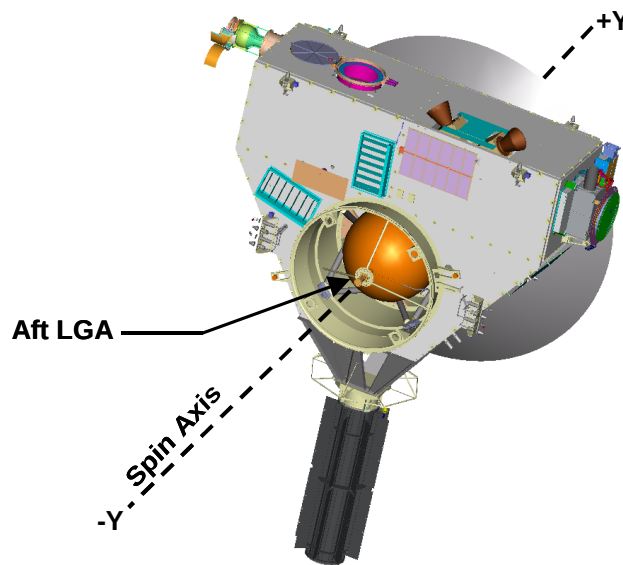


Figure 2: Aft Side of the New Horizon Observatory

The two low-gain antennas are used for near-earth operations and beacon mode/emergency operations for ranges less than 5-A.U. The 0.37-meter MGA antenna is used for beacon mode communications/emergency operations beyond 5-A.U. A highly efficient 2.1-meter parabolic reflector antenna (the HGA) is required to support the 600 bps 35-AU post encounter return link. This diameter reflector was selected after the NH antenna team performed a detailed alignment budget, which included effects due to thermal distortions on the spacecraft bus and the antenna system, dimensional tolerances, measurement knowledge of the antenna bore sight, ground station pointing errors, power margins, and antenna gain. This analysis showed that the HGA system and spacecraft spin-axis could accurately be aligned to within 0.2° . A 0.1° misalignment with the DSN ground station pointing due to ephemeris is added to this budget for a total alignment budget of 0.3° . A larger sized reflector antenna can be used on spin-stabilized spacecraft with enhanced definition, knowledge, and control of variables in the alignment budget; the downside is increased cost to the program.

The High Gain Antenna:

Background:

The New Horizon (NH) Concept Study Report states that the NH HGA system is required to support 600 bps at 35 AU post encounter return link for angles within 0.2° the spacecraft spin axis. The downlink system originally featured a 5-Watt SSPA and a 2.5-meter diameter, dual-shaped Cassegrain HGA. During Phase B and prior to the Preliminary Design Review, the NH antenna team performed a detailed alignment budget, which included effects due to thermal distortions on the spacecraft bus and the antenna system; dimensional tolerances, measurement knowledge of the antenna bore sight, and ground station pointing errors. The NH antenna team showed that the HGA coverage near the spacecraft spin axis would need to increase from $\pm 0.2^\circ$ to $\pm 0.3^\circ$ in order to satisfy the communication system requirements. Thus, the diameter of the main reflector was reduced from 2.5 to 2.1 meters to increase the beam width of the HGA in order to relax the alignment margin to 0.3 degrees. To offset the reduction in transmit EIRP; the SSPA was replaced with a 12 Watt TWTA. The smaller reflector also benefits the NH mission because it is lighter, cost less to manufacture, and is easier to handle during spacecraft integration.

Cassegrain Dual Reflector Description:

In order to achieve a well-collimated beam with Cassegrain optics, a concave paraboloid is employed for the large main reflector and a convex hyperboloid for the smaller sub-reflector. A geometrical interpretation of a classical Cassegrain design will show that a plane wave incident on the reflector system will focus the energy to a single point. Conversely, if the phase center of a feed horn is placed at this point, then the rays reflected by the sub and main reflector will be collimated into a well-defined main beam in the far field. This geometrical interpretation assumes that the feed horn is sufficiently small and the sub-reflector is located in its far-field region.

The directive efficiency of a reflector antenna system is generally the product of the

- (1) The fraction of the total power that is radiated by the feed, intercepted, and reflected by the subreflector ($\epsilon_{\text{feed_spillover}}$).
- (2) The fraction of the power incident from the sub reflector, intercepted, and collimated by the main reflector ($\epsilon_{\text{sub_spillover}}$).
- (3) Uniformity of the amplitude and phase across the antenna aperture ($\epsilon_{\text{amp_taper}}$, $\epsilon_{\text{phase_taper}}$).
- (4) Polarization uniformity of the field over the aperture plane (ϵ_{pol}).
- (5) Blockage efficiency ($\epsilon_{\text{blockage}}$).
- (6) Random surface errors over the reflector surface (ϵ_{rms}).
- (7) Position and tilt alignment errors of the feed and subreflector. ($\epsilon_{\text{alignments}}$).

Each of these terms can have a significant effect on the efficiency of the NH reflector system. Appropriate selection of Cassegrain reflector parameters and PO synthesis of the reflector surface, high efficiency can be achieved.

Designing for High Directive Efficiency:

A sub-reflector provides an additional degree of freedom for achieving high efficient antenna performance. The directive efficiency of the reflector system is improved by modifying the shape of one or both reflecting surfaces. For the NH mission, it is desirable to reshape both reflecting surfaces to achieve uniform amplitude and phase distribution across the radiating aperture. One approach to optimize the directive efficiency of the HGA system is to reshape the sub-reflector surface until the amplitude across the antenna aperture is nearly uniform and the aperture phase is corrected with the main reflector surface. This approach is referred in the literature as geometrical optics (GO) shaping. This algorithm improves the antenna directivity but the performance is not optimal due to limits with ray optic assumptions at microwave frequencies. Some of the effects not modeled with GO include: diffraction effects, feed/sub-reflector interactions, struts, and blockage. These terms can be modeled with a physical optics (PO) approximation of the induced current density. Once the current is known, the far field pattern of the antenna is determined by integration. The theory of physical optics is well developed and documented in technical journals.

One reason PO models are traditionally not used for designing shaped reflector surfaces is slow execution times and the optimization process usually requires large number of iterations before convergence is achieved. In addition, it is difficult to derive a straightforward procedure to efficiently iterate both reflector surfaces. A research group (Antenna Software Limited, (ASL)) in England recently developed a technique to that addresses these problems and their strategy is described in Reference 1. A commercial software tool called AXIPO was also developed and used to design the NH HGA reflector surfaces. This tool was specifically developed to optimize an axial symmetrical single feed dual shaped reflector antenna design, which is the architecture of the NH HGA system.

The HGA Design:

One design challenge with dual reflector antenna systems is the ability to balance conflicting RF, mechanical, and structural requirements. Reflector designs are often restricted by factors such as system mass, package volume, feed horn fabrication feasibility, reflector size, and cost. The NH communications system has established that the HGA must provide a minimum antenna gain of 42 dBiC for angles within $\pm 0.3^\circ$ of the spacecraft spin axis in order to support 600 bps 35-AU post encounter return link. This requirement could be achieved with a standard Cassegrain reflector design but the gain margin at angles within $\pm 0.3^\circ$ from the spacecraft spin axis is less than 0.5 dB. The unshaped reflector system is completely described by the parameters listed in Table 1.

Table 1: Baseline Cassegrain Reflector Geometry

Parameter	Value
Focal Length, F	0.756 meters
Reflector Diameter, Dm	2.1 meters
F/Dm	0.36
Sub Reflector Diameter, Ds	38 cm
Ds/Dm	0.18
Feed Illumination, θ_e	26 degrees
Sub Reflector Interfocal length, 2f	46 cm
Distance: Reflector vertex to feed horn phase center, Lm	30 cm
Distance: Sub Reflector apex to feed horn phase center, Ls	35 cm
Feed Horn Diameter	15 cm
Feed Horn Length (includes polarizer)	34 cm

This is achieved with high amplitude taper (18 dB) across the sub reflector; the taper for an unshaped reflector design is typically -12 dB. Cassegrain optics is also attractive solution for the NH mission because the feed can be placed close to the vertex of the main reflector, further minimizing cable insertion loss.

The final NH HGA design features a 2.1-meter diameter main reflector. A 0.38-meter diameter sub reflector (~ 11 wavelengths) directs the radiation from the feed to the main reflector. Experience has shown that the sub-reflector diameter must be at least 10 wavelengths in order to minimize edge diffraction effects. Here a larger sub-reflector size is non-optimal because it introduces excessive shadowing/blockage. There are two blockages that are considered: shadow of the sub reflector and shadowing. The 26-degree feed illumination angle positions the feed so its input is positioned just below the vertex of the main reflector.

A 15 cm diameter feed horn positioned about 35 cm below the sub reflector apex, provides 18 dB illumination taper across the sub reflector, resulting in a small feed spillover loss. A compromise usually exists between feed-spillover and aperture illumination efficiencies. Since the reflector surfaces are synthesized, simultaneous optimization was possible.

Forward Antenna System Performance:

In this section the measured radiation and VSWR performance of the antennas in the forward antenna assembly, which consists of a LGA, MGA, and a HGA, will be reported and compared to the requirements levied by the RF communication systems. All radiation and VSWR measurements for this subsystem were performed in Columbus Ohio using the compact antenna range at the ElectroScience Laboratory (ESL). A picture of the antenna measurement setup inside the ESL facility is shown in Figure 3. The performance of each antenna is shown in Figures 4 through 13. All of the antennas meet or exceed the performance required by the communication system.

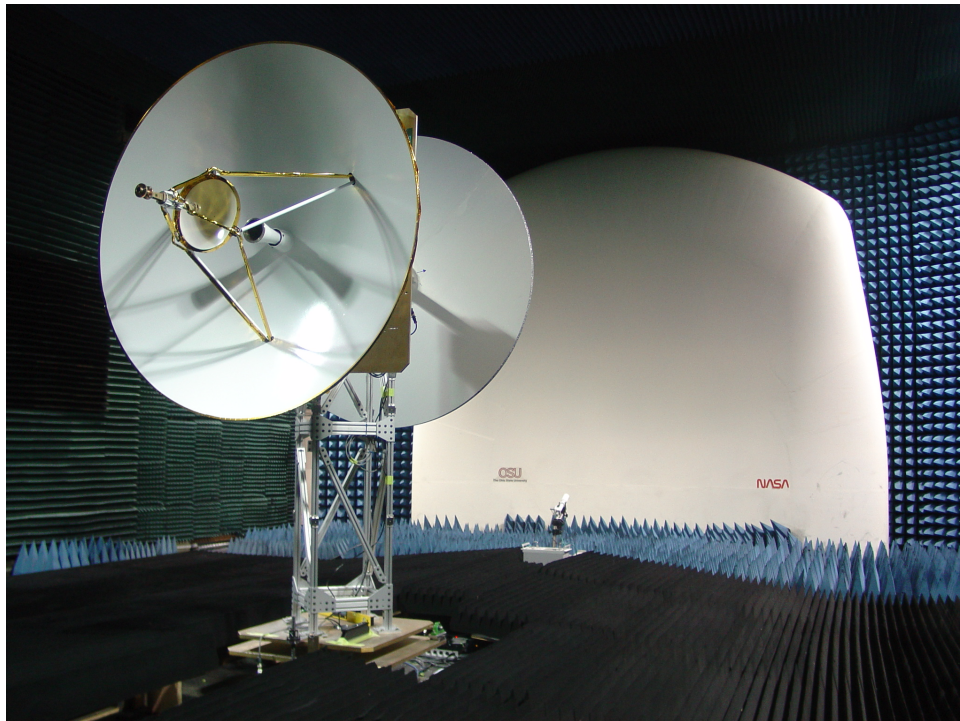


Figure 3: Measurement of the Forward Antenna System at ESL

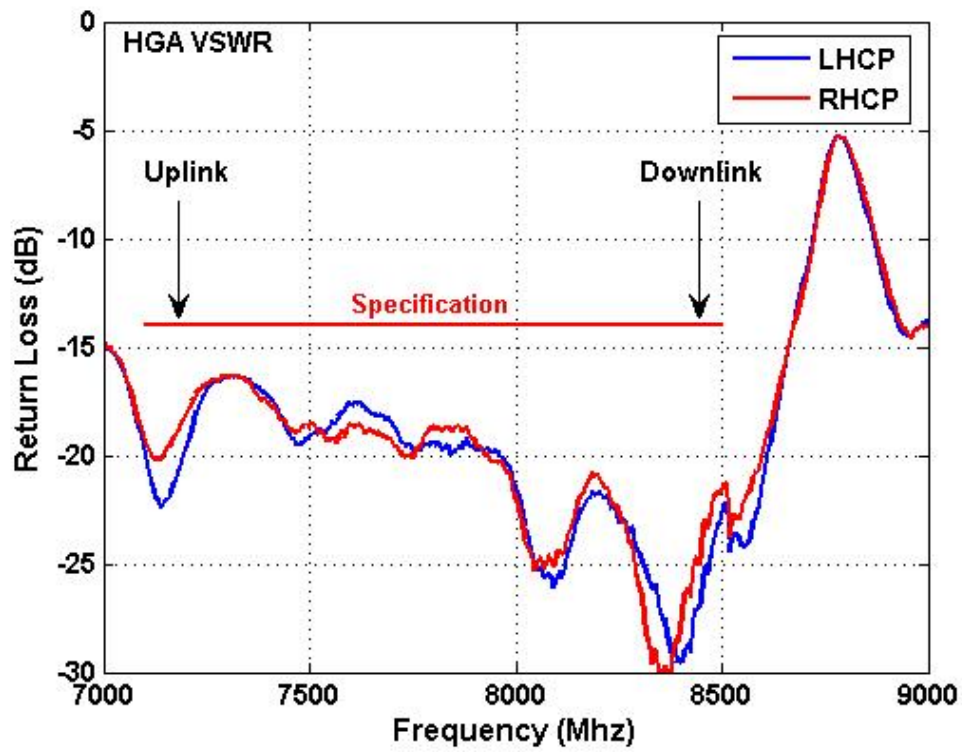


Figure 4: VSWR Performance for the HGA

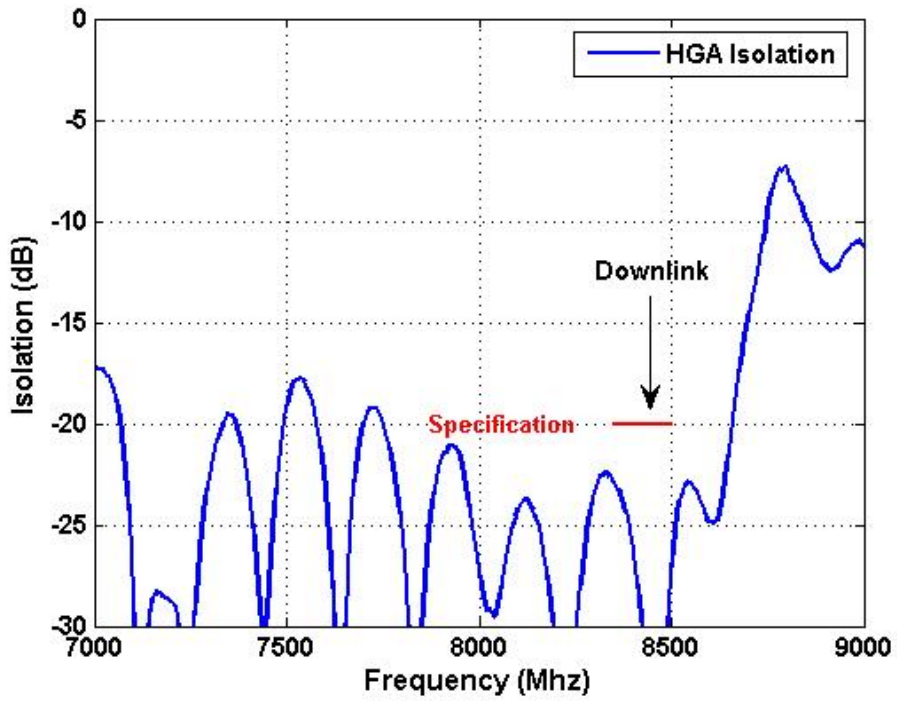


Figure 5: Isolation Performance for the HGA

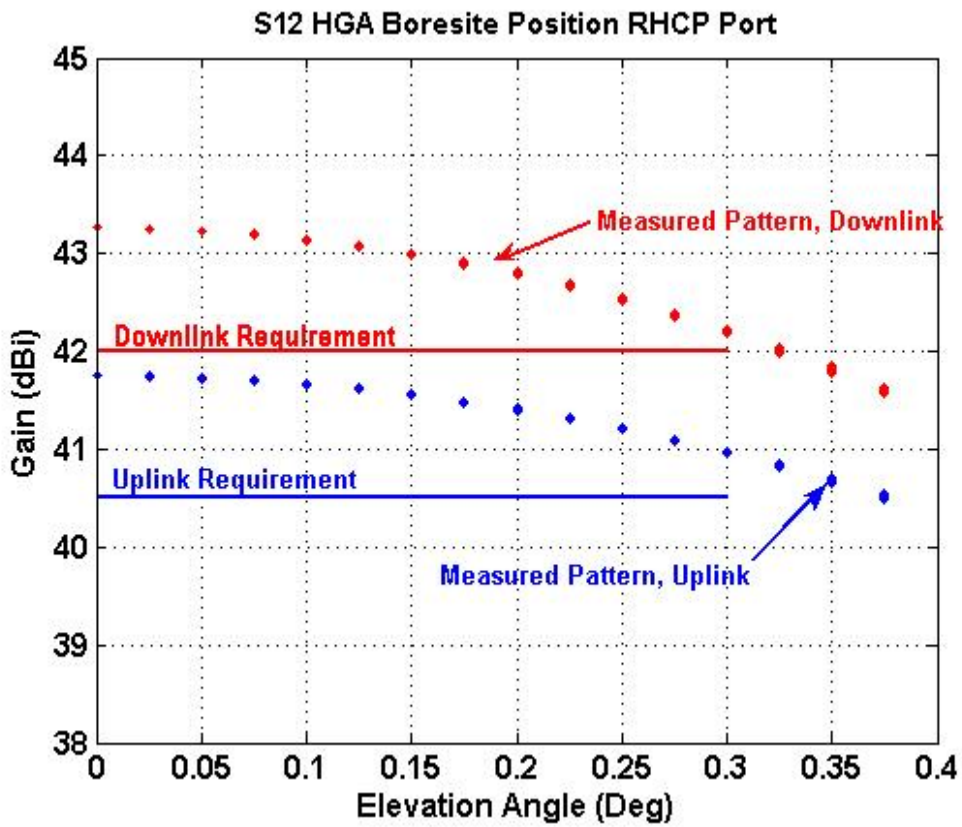


Figure 6: Measured Gain versus Angle for the 2.1 meter HGA, RHCP

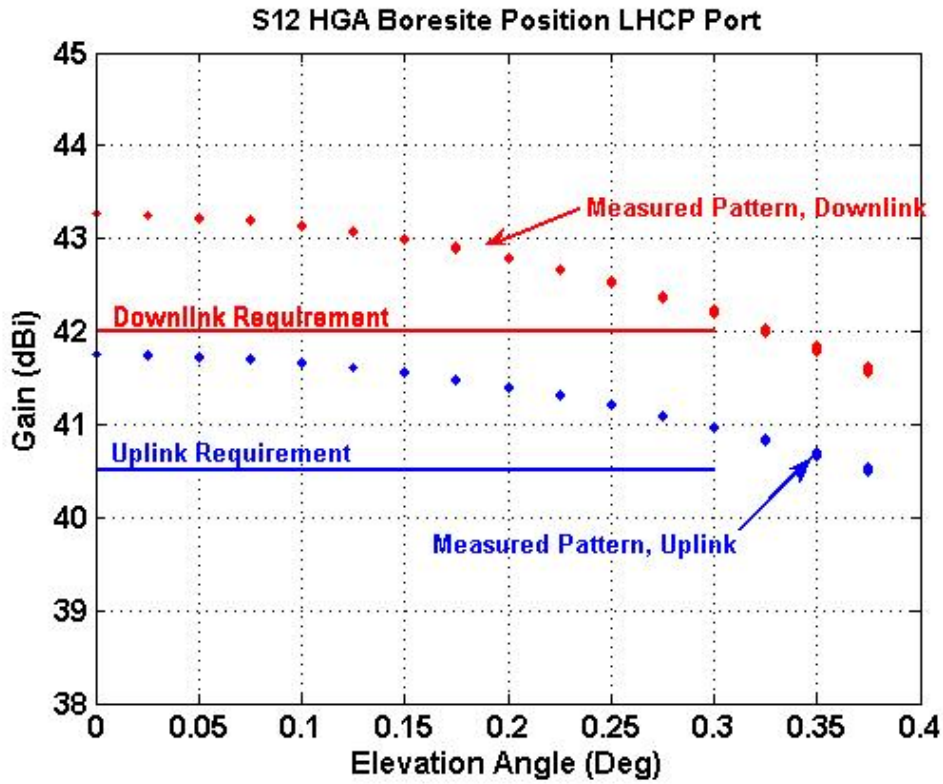


Figure 7: Measured Gain versus Angle for the 2.1 meter HGA, LHCP

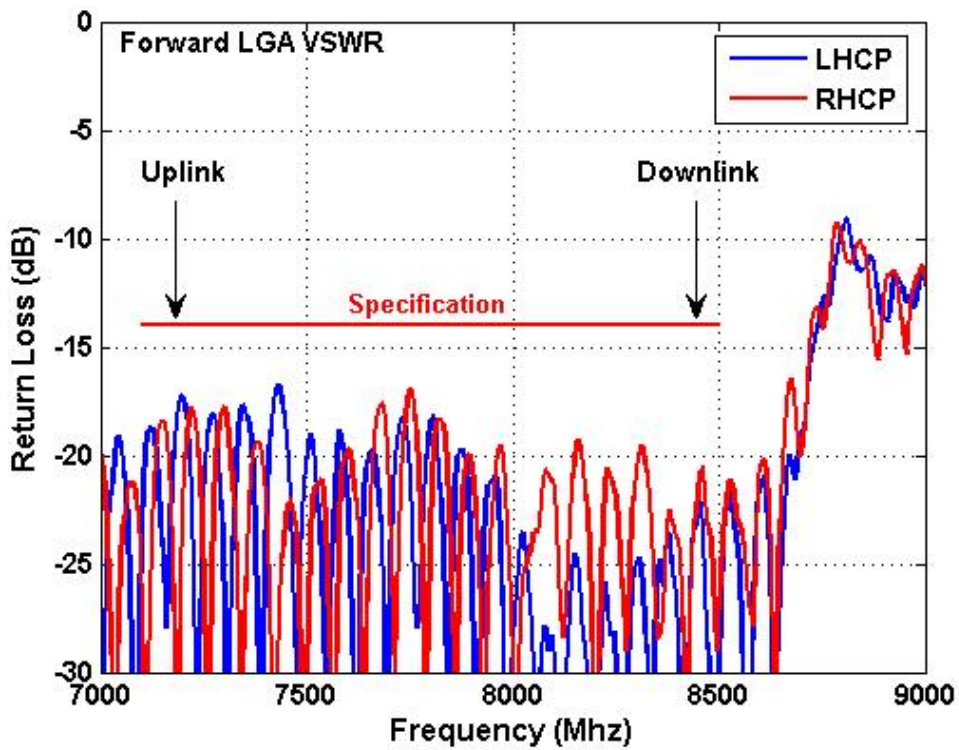


Figure 8: VSWR Performance for the Forward LGA (cables included)

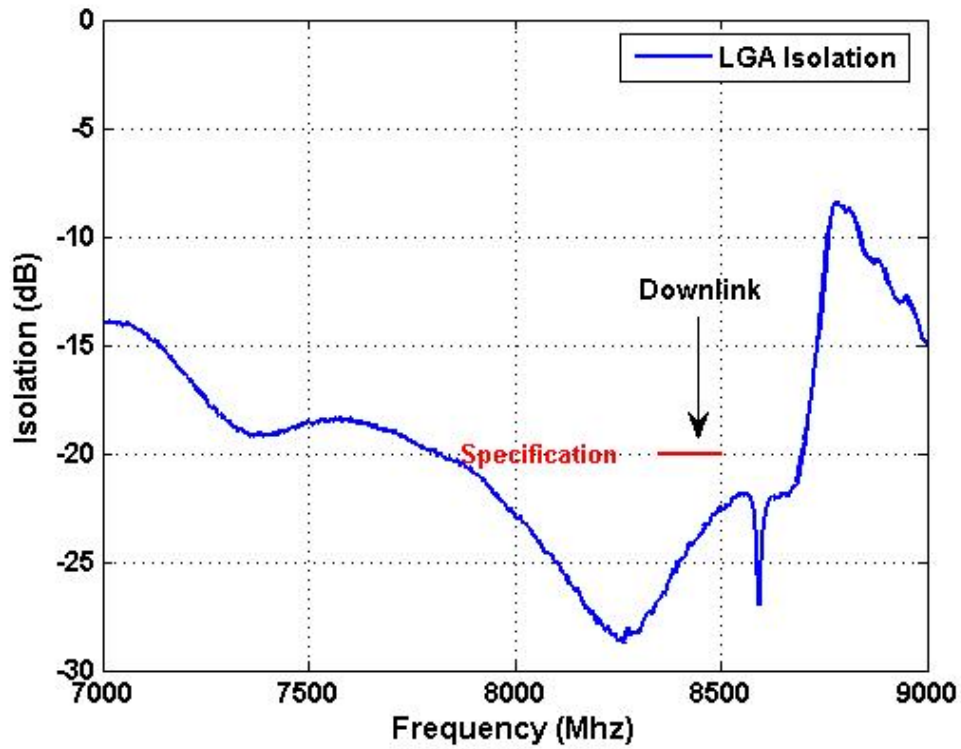


Figure 9: Isolation Performance for the Forward LGA

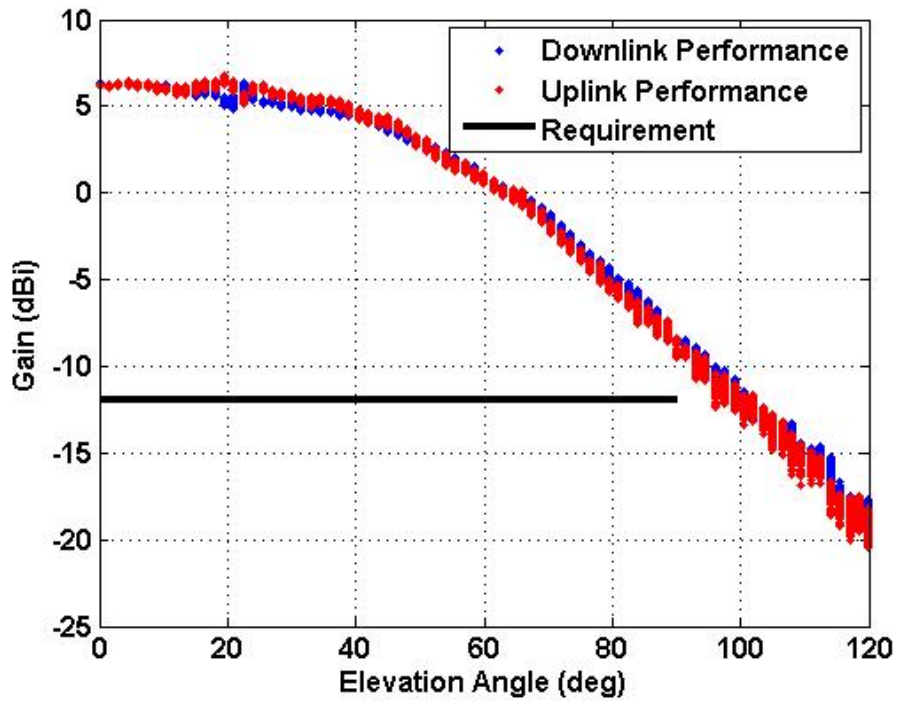


Figure 10: In-situ Gain Performance versus Angle for the Forward LGA

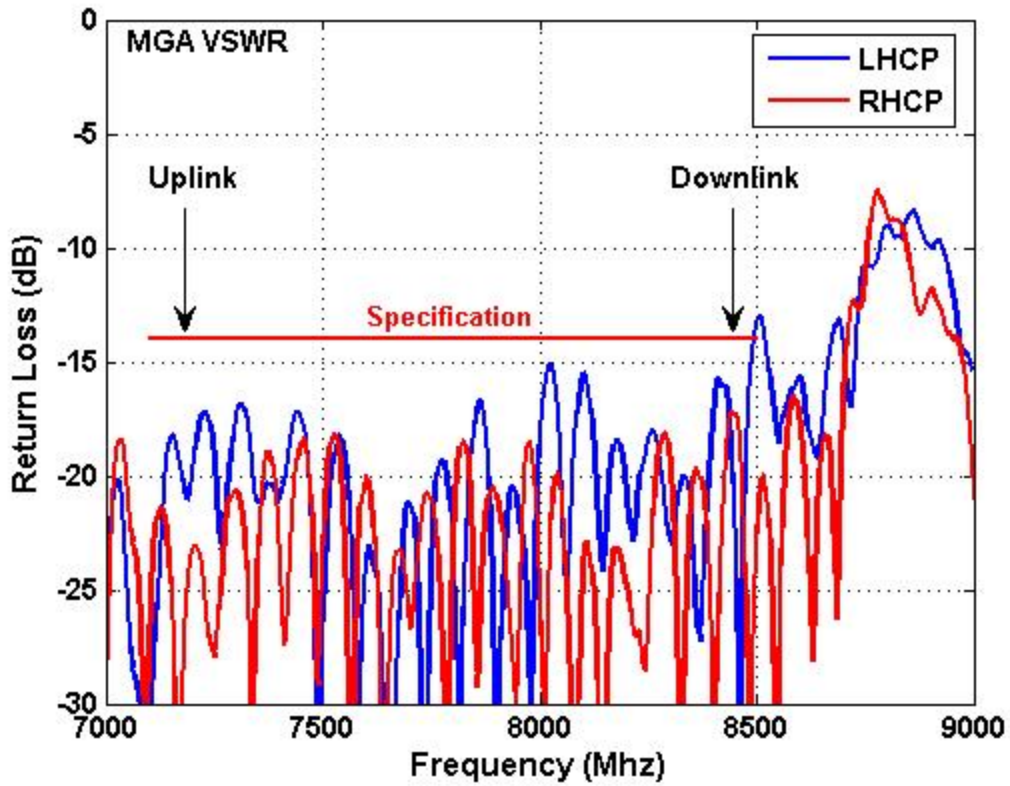


Figure 11: VSWR Performance for the MGA (cables included)

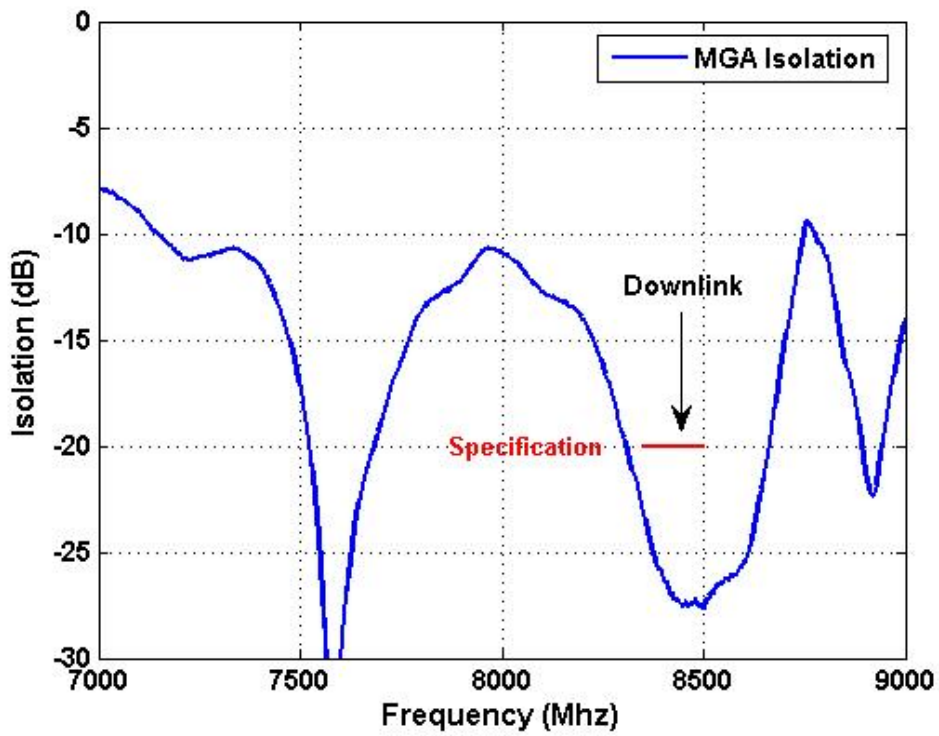


Figure 12: Isolation Performance for the MGA

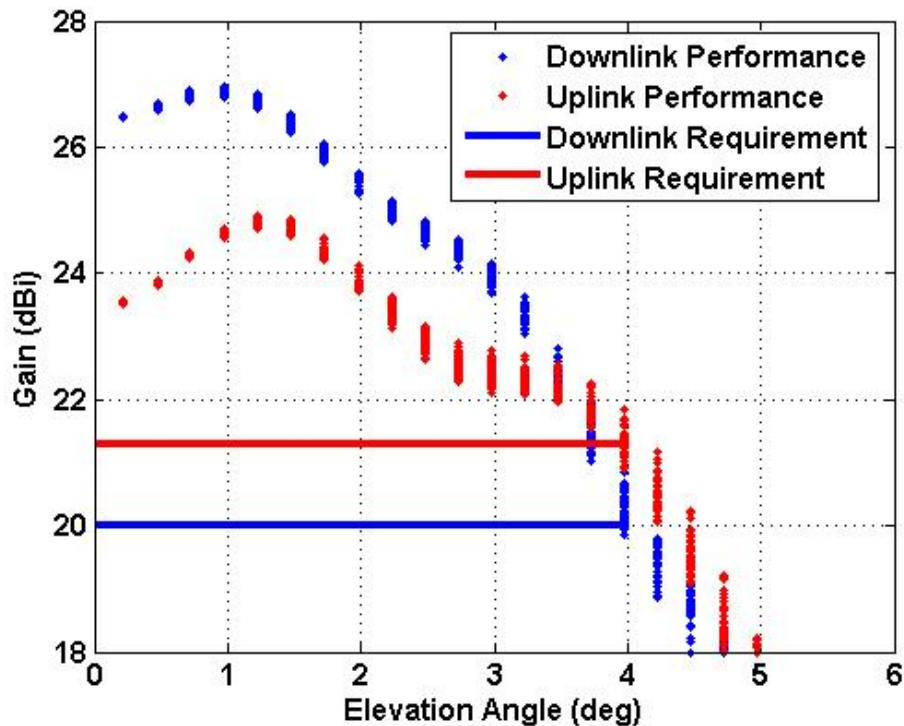


Figure 13: In-situ Gain Performance versus Angle for the MGA

Alignment Measurements:

In order for the HGA system to meet its part of the communication system mission requirements, the HGA boresight alignment is required to be within 0.2° to the spacecraft spin axis. A detailed alignment error budget was developed to keep track of the terms that could misalign the antenna boresight position. A potential large term in this error budget is the accuracy in which the electrical boresight position is measured. In order to meet the above system alignment requirement 0.05° was budgeted for this error. As will be shown during this section, the RF boresight error of the HGA antenna system is approximately 0.025° . The primary measurement error source ended up being the physical misalignment between the RHCP and LHCP beam position, which was 0.04° degree. The physical difference between the two beams was split when alignment measurements were performed. In this section, only the RF portion of the alignment procedure will be discussed. An overview of the optical measurement procedure will be discussed here but the details related to (1) the optical measurement techniques, (2) translating the RF boresight position to an optical reference, (3) the processing of the measured optical data, and (4) the final boresight error budget will be discussed in a separate memorandum.

Alignment Plan Overview:

The alignment test program for the NH HGA system was designed to: (1) reference the RF boresight to a physical mechanical reference, (2) qualify the mechanical system

design by measuring the relative alignment of the HGA feed, sub-reflector and primary reflector components at cryogenic temperature, and (3) align the RF boresight to the observatory coordinate system. Again it is noted that this memorandum only addresses the RF measurements performed in support of the overall alignment of the HGA system.

Originally, the alignment measurement plan relied entirely on measuring attached optical references (i.e. mirrors) for vector metrology. This approach proved to be unreliable and sensitive to the GSE plate configuration that the antenna was attached to during measurements. For these reasons the optical cube approach was abandoned, late in the program, in favor of attaching coordinate targets to the reflector surface and using multiple-Theodolite coordinate triangulation techniques to measure the dish axis. To utilize this set of coordinate targets as a known “reference”, for measuring the antenna boresight, a coordinate system had to be consistently identified from the raw point data. This was achieved by fitting the nominal dish shape to the measured targets, defining a HGA axis of symmetry. In many ways, this is a superior reference, as compared to the optical cube surfaces, because of its tight correlation with the actual surface of the HGA.

The coordinate system of the HGA boresight axis is then mapped to the spacecraft spin axis by measuring the axes of the incident plane wave, which is equivalent to the spacecraft spin axis. The incident plane wave axis is defined by the peak response/return from the RCS plate. The theodolites stands were left in place between RCS plate and NH HGA measurements, providing a common reference coordinate system for each measurement. The vector difference between these measurements is the desired HGA boresight mapped into the coordinate system during spacecraft integration.

During spacecraft integration, shims under the HGA mounting feet were used to fine-tune the angular alignment of the RF bore-sight to the spacecraft spin axis, using the coordinate targets as our mechanical reference. An iterative process of shimming and surface measurement was used to bring the HGA boresight into alignment with the spacecraft coordinate system (within $\sim 0.008^\circ$). No provisions for possible movement due to thermal effects during the mission are incorporated into the antenna internal alignment or antenna to spin axis alignment.

Alignment Measurement Setup:

The primary goal for any antenna/alignment measurement setup is a flat phase front (i.e. plane wave) across the test zone, which is achieved in a compact antenna range by placing the phase center of the range feed at the focus of the compact range reflector. It is noted that since the phase center of the range feed changes with frequency, the direction of the phase front will change with frequency across the test zone. To minimize this variation, a Potter horn was selected for the range feed because its phase center variation is small over the frequency band of operation. As it turns out, the shift in the plane wave direction is a non issue for alignment measurements because the relative vector orientation between the RCS plate and NH HGA at a single frequency (8435 MHz) is the desired measurement term.

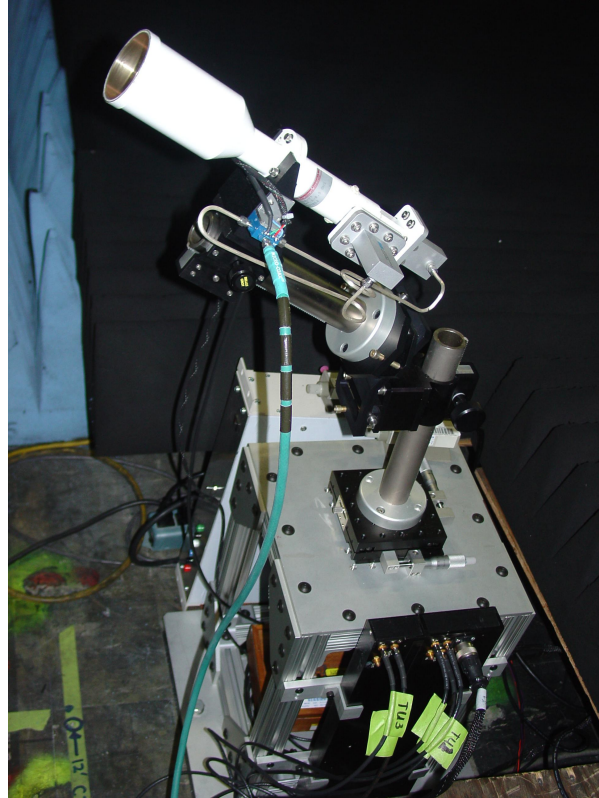


Figure 14: Compact range feed stand showing various degrees of freedom

A flat phase front is achieved when the phase slope across the aperture is zero. To achieve this measurement goal in a timely fashion the range feed stand was equipped with precision micrometers on a X/Y/Z translation stage, as shown in Figure 14. This mechanism was used to iteratively adjust the physical position of the feed horn until the phase slope was flat across the entire test zone. The fields in the test zone were measured using a 96-inch linear translation stage and a broadband, low-gain horn antenna (AEL-1498), as shown in Figures 15a and 15b. The final probe measurements for horizontal polarization at 8435 MHz are shown in Figure 16a, and 16b, when the linear translation stage is oriented vertically and horizontally, respectively. This figure shows that the range feed is well aligned to the range reflector system. Vertical polarization measurements were also performed but not shown because the results are nearly identical.

RCS Plate Measurement Setup and Data Processing:

The plane wave orientation in the compact antenna range is the next step in our process to measure the boresight position of the HGA. The probe measurements discussed in the previous section demonstrated that fields in the aperture plane were sufficient for the boresight measurement. In this section, the reflection measurement from a 2.1-meter circular test plate will be discussed. The test plate for the remainder of this memorandum

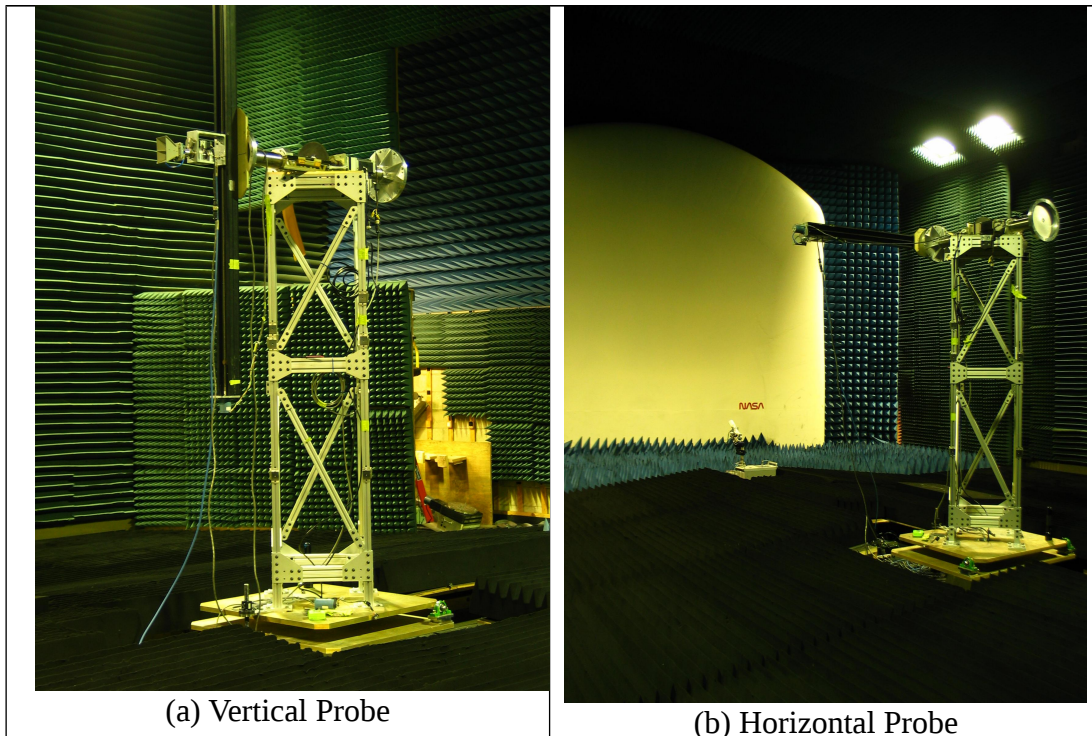


Figure 15: Field Probe Test Setup

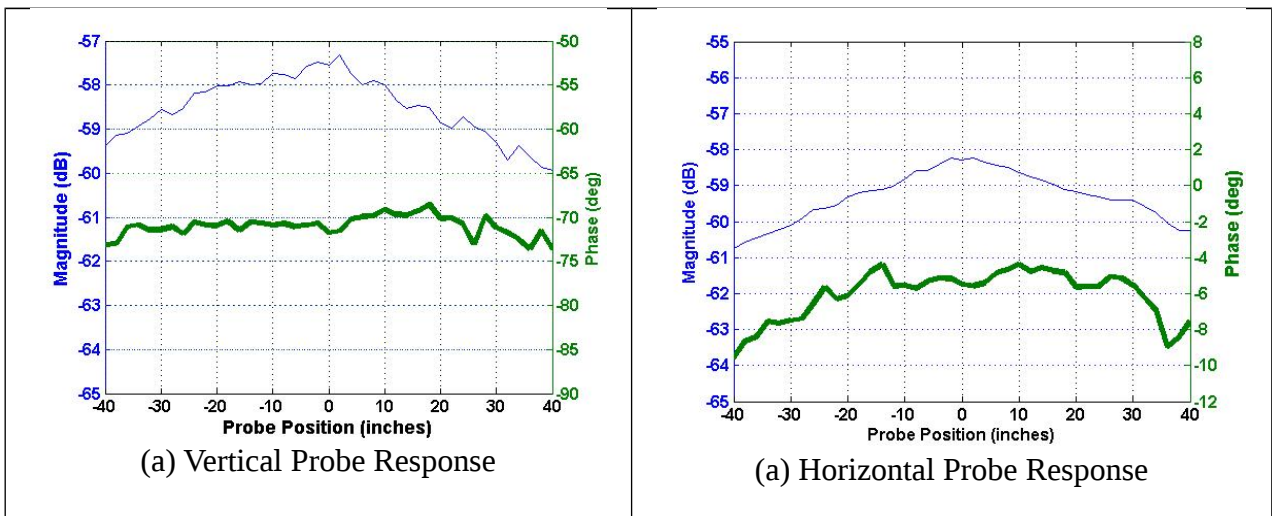


Figure 16: Amplitude (blue) and phase (green) response across test zone.

will be referred to as the radar cross section (RCS) plate. The purposes of the 2.1-meter diameter RCS plate are: (1) act as a vector reference for the plane wave orientation in the compact range facility and (2) gain reference for the NH HGA.

The RCS plate is a convenient gain reference because the peak reflection return is directly related to the gain of the AUT, a subject of another memorandum. This measurement is important here because in the test zone, a 3-dB amplitude taper is present across the test zone, as shown in Figures 16a and 16b. Since the NH HGA is designed

with a uniform aperture distribution, a gain comparison technique using a gain reference horn would establish a conservative gain value for the NH HGA, as much as 1 dB. This effect is well documented in the literature and corrections to the gain level can be derived using rigorous electromagnetic computations. During the program, APL and OSU developed a simple technique to directly measure the HGA gain using the RCS plate as the reference. Since the area of the plate is known and identical to the HGA diameter, a direct comparison between the two responses will reveal the exact gain of the NH HGA, without any additional computations and was used during this measurement campaign to derive the gain performance of the HGA.

A drawing of the actuated test stand with the RCS plate and NH HGA installed is shown in Figure 17. This test stand was developed to provide precision positioning of the antenna (and plate) with three degrees of freedom; the degrees of motion and respective labels are illustrated in this figure. During the alignment measurement campaign, the nominal measurement parameter for each axis is listed in Table 1 and shows that step/scan measurement (elevation, tilt) sequences were performed at two azimuth positions: 0° and 180° .

Before RCS plate backscatter measurements were performed, the plate was mechanically aligned to the azimuth spin axis of the NH test stand, using a digital micrometer to measure the front surface at a fixed radial distance, as shown in Figure 18. Small shims were inserted between the plate and test stand mounting interface until the plate was mechanically aligned within 0.01° . During this measurement a small surface distortion across the plate surface was observed and verified later using a laser radar metrology system to measure the “flatness of the RCS plate. A plot of the surface distortion across the RCS plate is shown in Figure 19. The surface distortion is small (less than 0.020 inches peak), especially when compared to the free-space wavelength, ~ 1.4 inches at the downlink frequency (8435 MHz). Its effect on alignment is also minimal. In fact this error term is essentially eliminated because the RCS boresight position (tilt, elevation) was selected to be the mean of two backscatter measurements (Azimuth: 0° , 180°).

Figure 20 is a surface/contour plot of the plate backscatter response after the plate was mechanically aligned and when the plate is at 0° in azimuth for 8435 MHz. In this plot the contour levels are relative to the beam peak, in 0.5-dB increments. Instead of selecting the peak response of the RCS plate to determine the plane wave vector (tilt, elevation) the 2.5-dB contour, relative to the peak, is used. This approach is ideal because it (1) averages any deleterious effects a local maximum in the plate response might produce, (2) is easy to program a software algorithm to calculate the boresight position as a function of frequency, and (3) provides immediate feedback to the test conductor when a problem in the measurement setup exists.

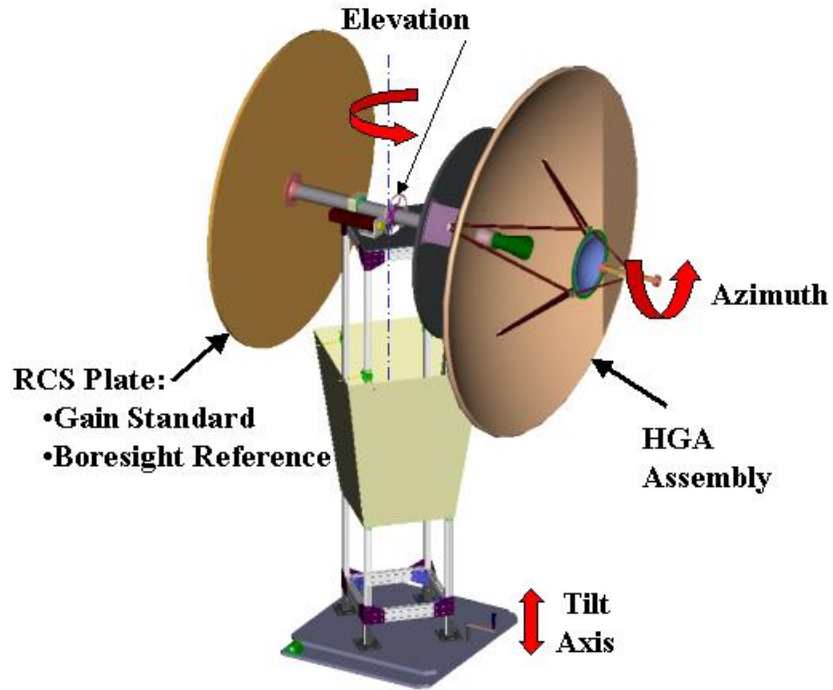


Figure 17: NH Test Stand for the Forward Antenna System Measurements

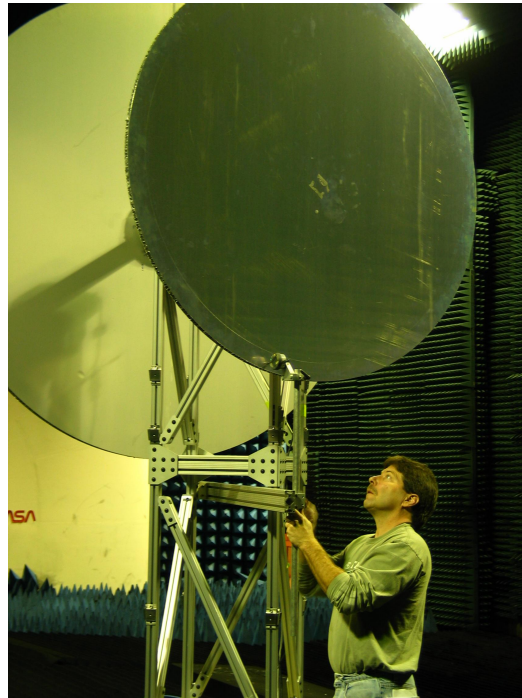


Figure 18: Mechanical Alignment of RCS Test Plate to Test Stand Azimuth Axis

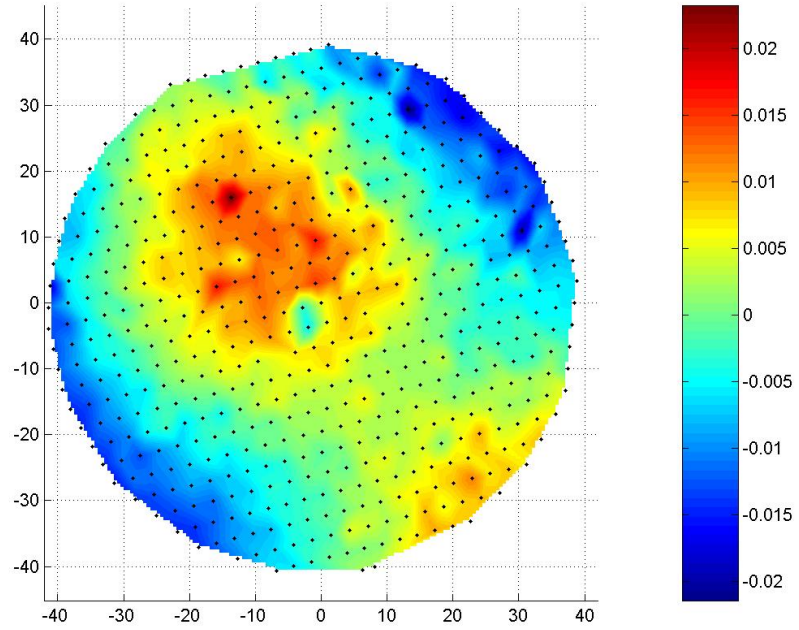


Figure 20: Surface Distortion for 2.1-meter RCS Test Plate (plot units are inches)

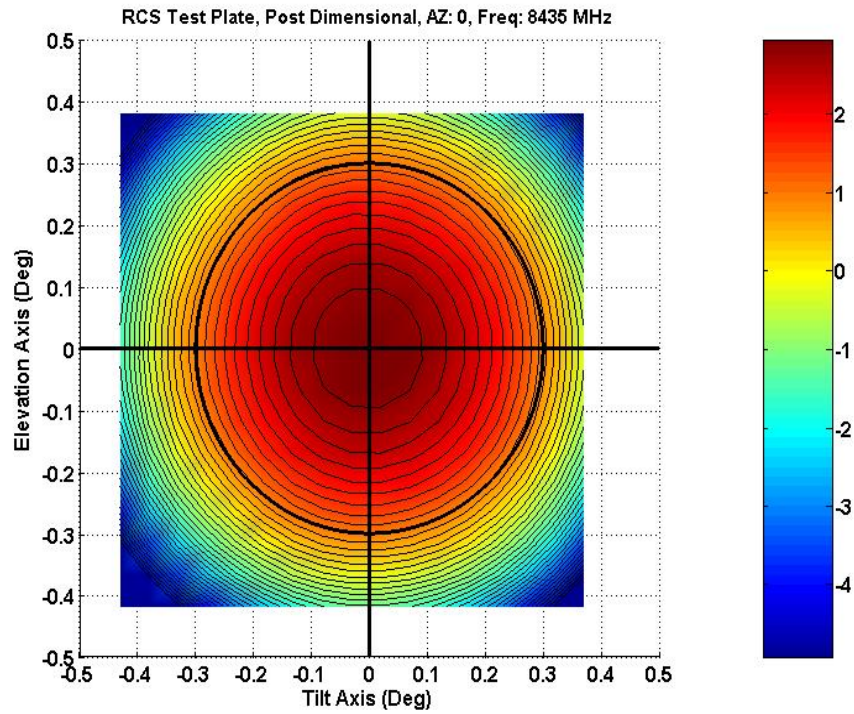


Figure 20: Backscatter Response for 2.1-meter RCS Test Plate

NH HGA Alignment Measurement Setup:

The setup for the HGA is more complicated than the RCS setup because a physical surface is not available to align the beam position to the azimuth spin axis. Instead the pattern response of the HGA, using the step/scan parameters in Table 2, for azimuth positions 0° and 180° and for both antenna polarizations (RHCP, LHCP) is required to determine and align the peak response of the antenna to the spin axis of the test stand. As it turns out, the baseline HGA boresight was not far from the test stand spin axis: 0.0325° in the elevation axis and 0.05° in the tilt axis. Again, shims were used to align the HGA beam peak to the azimuth axis of the test stand; the values of shims are listed in Table 3. There are a total of eight 0.25-28 mounting lugs on the test stand and the number indicated in the first column is the label assigned during the measurement campaign. Figure 21 is a color plot of the HGA response for the step/scan parameters in Table 2 after alignment when the HGA was at 0° in azimuth. This plot shows that the pattern is circularly-symmetric, as expected.

Table 2: Motion Control Parameters for the HGA Response Measurement

Scan Axis:Tilt	Step Axis: Elevation	Fixed Axis: Azimuth
$\pm 1.5^\circ$	$\pm 1.5^\circ$	$0^\circ, 180^\circ$

Table 3: Shim Values for Alignment of HGA to the test stand

Test Stand Label	Shim Value (inches)
1	0.001
2	0.000
3	0.003
4	0.007
5	0.010
6	0.011
7	0.009
8	0.004

To demonstrate the NH HGA is well-aligned to the azimuth axis of the test stand, the boresight position (elevation, tilt) as a function of frequency for both input HGA ports and for two azimuth positions is shown in Figure 22a and 22b. It is noted that the boresight position between the +Z and -Z ports of the HGA, in the elevation axis, is different by approximately 0.04° . This shift was a little surprise but makes sense now because the polarizer is asymmetric in this axis. This difference was split when dimensional and cube alignment measurement was performed; and is the largest error term for RF bore-sight determination.

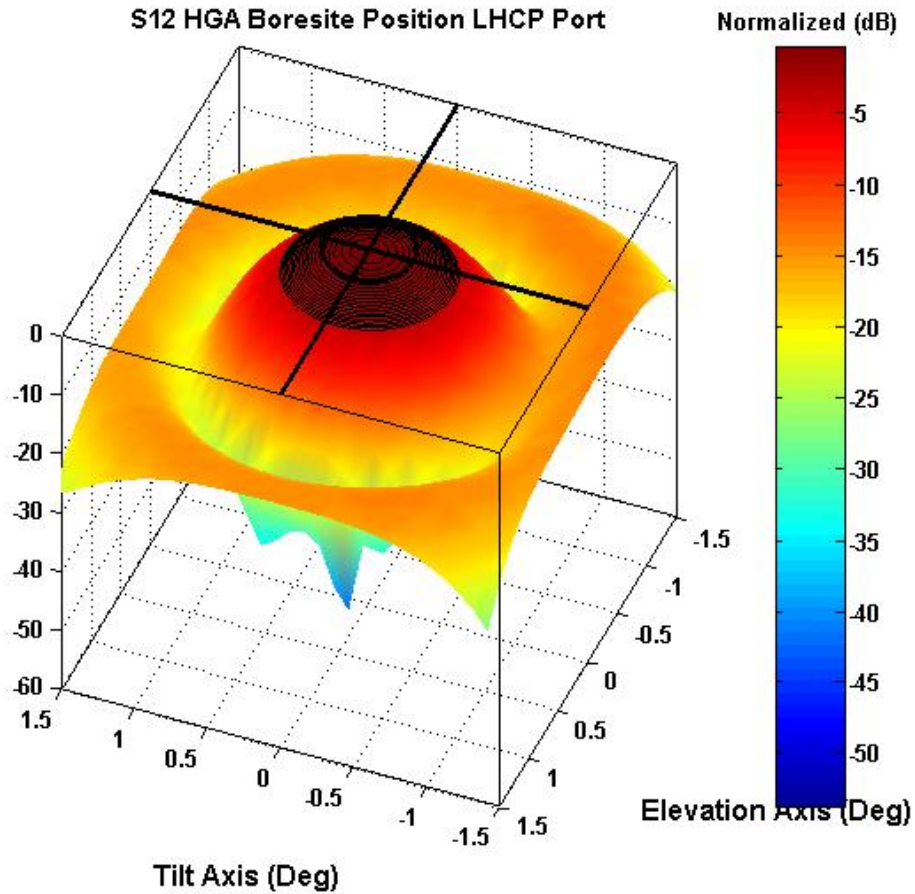


Figure 21: Color plot of the HGA response for the step/scan parameters in Table 2 after alignment when the HGA was at 0° in azimuth

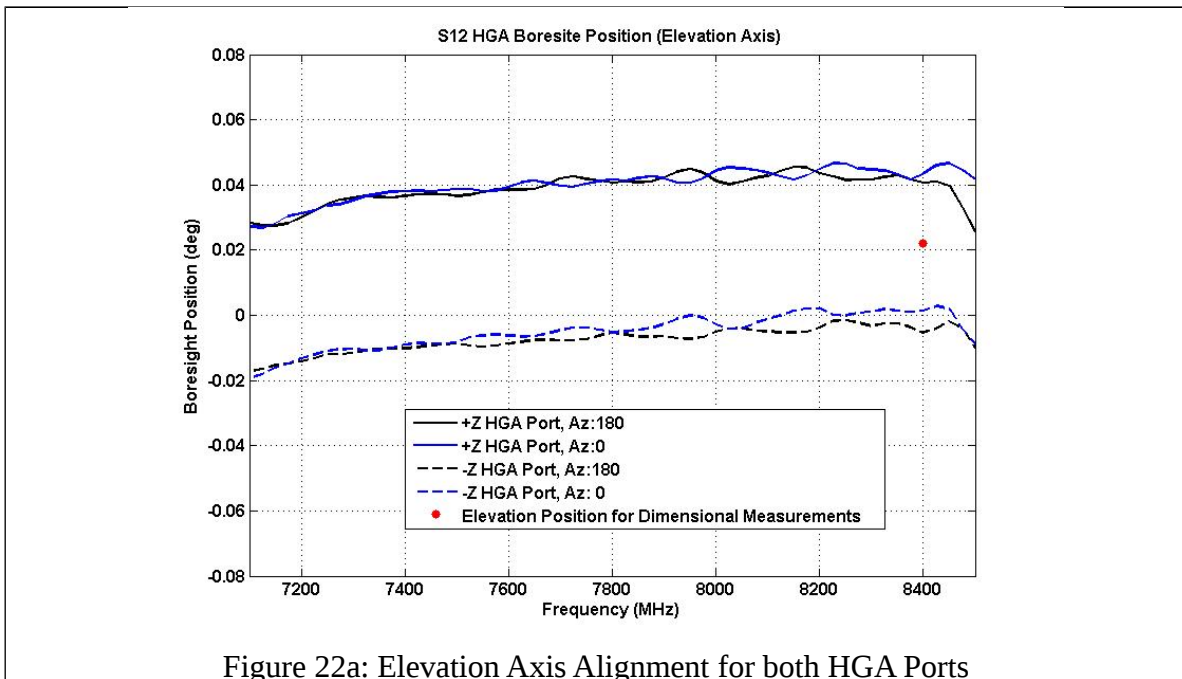
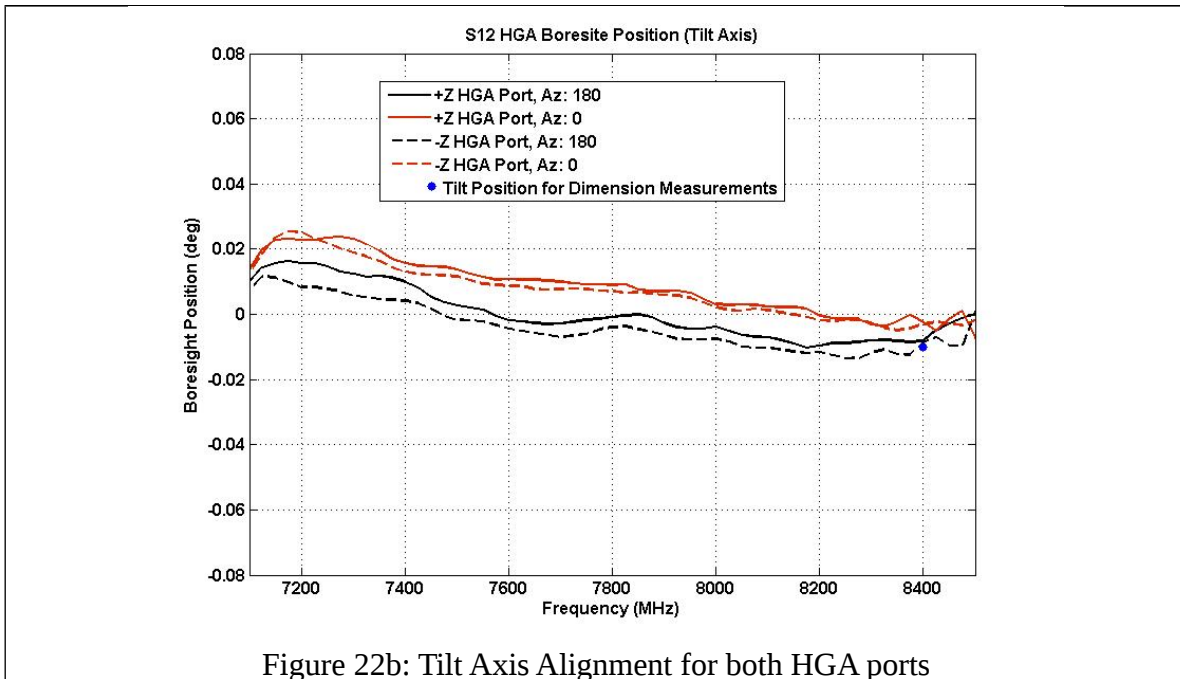


Figure 22a: Elevation Axis Alignment for both HGA Ports



Alignment Measurement Campaign:

The alignment measurement data campaign is a combination of RF and optical alignment measurements, as shown in Table 4. This table lists the sequence of events that occurred in early March, which is when the final boresight of the HGA was performed. The overarching goal of this measurement sequence is the transfer the RF boresight to a mechanical reference, which will be used for spacecraft integration activities. During the alignment measurement campaign, it is important that the test stand with the RCS test plate and forward antenna assembly remain mechanically stable, which implies that the boresight position is repeatable. As indicated in Table 4, the boresight position, for both test articles, was measured versus frequency between each optical alignment procedure. The RF measurement step/scan parameters to confirm the boresight positions are tabulated in Table 5. It would be overwhelming to the reader to plot the step/scan results for each azimuth angle. Instead, the processed boresight position (tilt, elevation) versus frequency, using the measured data, for the HGA and RCS test plate is used, as shown in Figures 23a through 24b. Recall that two azimuth angles are required to derive the final “processed” boresight position, which is wrapped into the data indicated in these figures. For the interested reader, the boresight position for RCS test plate for each azimuth position (0, 180) throughout the alignment measurement campaign is tabulated in Table 6. Based on these data, the test setup was quite stable during the alignment measurement campaign, which was the goal.

Table 4: Alignment Measurement Campaign Sequence

Sequence	Date	Measurement
1	March 15 (PM)	Determine Boresight Position of HGA and RCS Plate
2	March 16 (AM)	Repeat (1)
3	March 16 (mid-day)	Optical Cube Measurements
4	March 16 (PM), March 17 (AM)	Determine Boresight Position of HGA and RCS Plate
5	March 17 (mid-day)	Dimensional Measurements
6	March 17 (PM), March 18 (AM)	Determine Boresight Position of HGA and RCS Plate

Table 5: Motion Control Parameters for the RCS Response Measurement

Scan Axis:Tilt	Step Axis: Elevation	Fixed Axis: Azimuth
$\pm 0.5^\circ$	$\pm 0.5^\circ$	$0^\circ, 180^\circ$

Table 6: Summary of Plate Boresight Position during Alignment Measurement Campaign

Boresight Position of RCS Plate, Pre Dimensional		
Azimuth (deg)	Elevation (deg)	Tilt (deg)
0	180.011	0.226
180	180.019	0.231
Average	180.015	0.229
Boresight Position of RCS Plate, Post Dimensional		
Azimuth (deg)	Elevation (deg)	Tilt (deg)
0	180.016	0.230
180	180.018	0.229
Average	180.017	0.229
RCS Plate Orientation of RCS Plate during Dimensional Measurement		
Azimuth (deg)	Elevation (deg)	Tilt (deg)
0,180	180.015	0.229

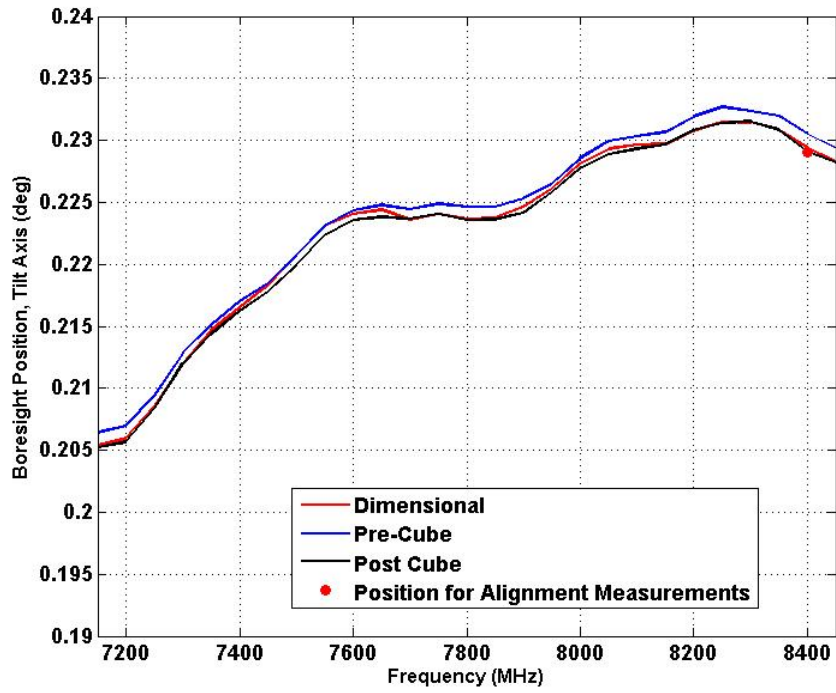


Figure 23a: RCS Plate Boresight Position, Tilt Axis versus Frequency

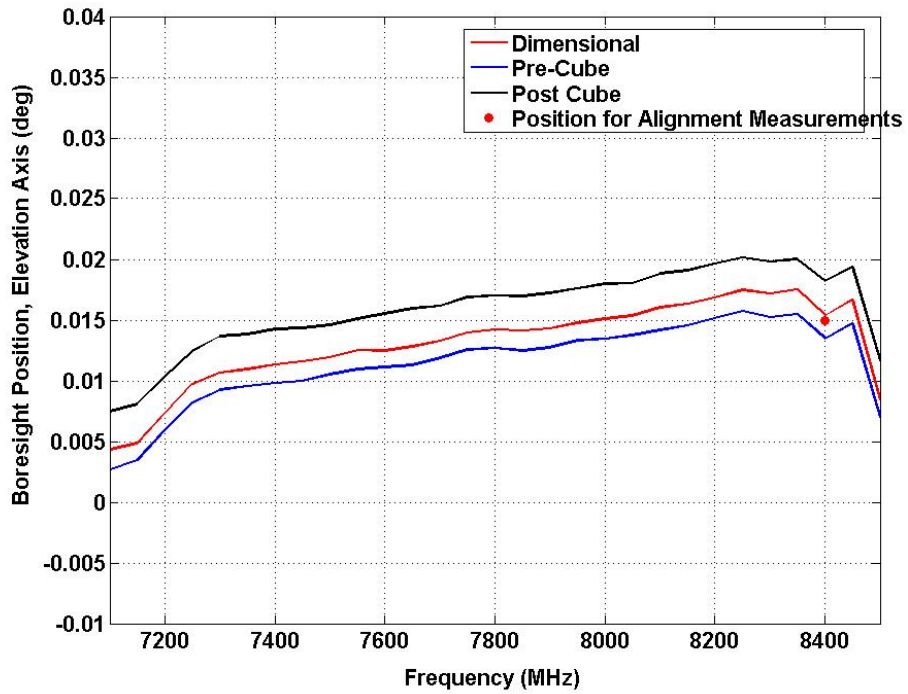


Figure 23b: RCS Plate Boresight Position, Elevation Axis versus Frequency

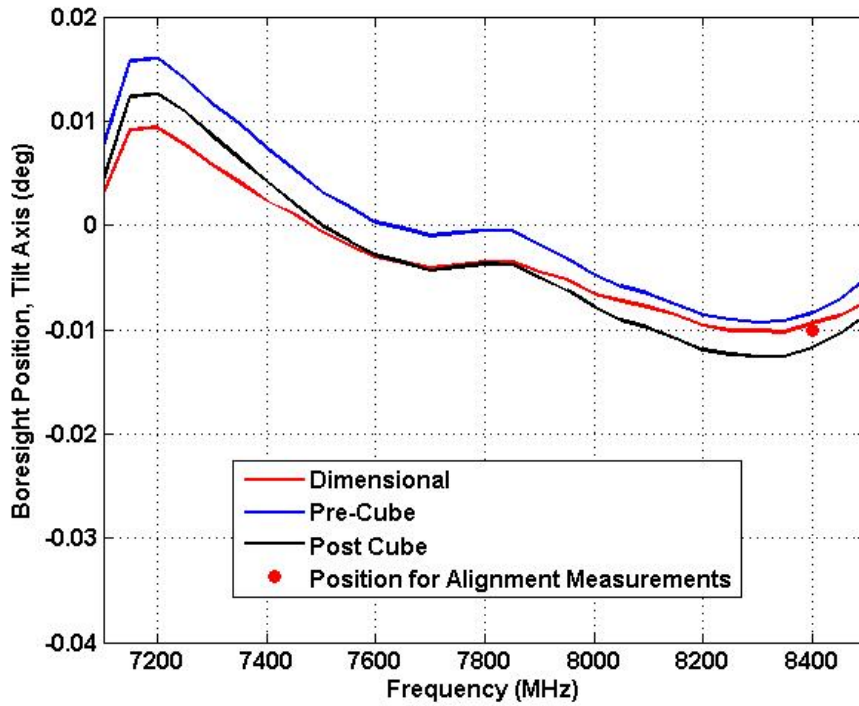


Figure 24a: HGA Boresight Position, Tilt Axis versus Frequency

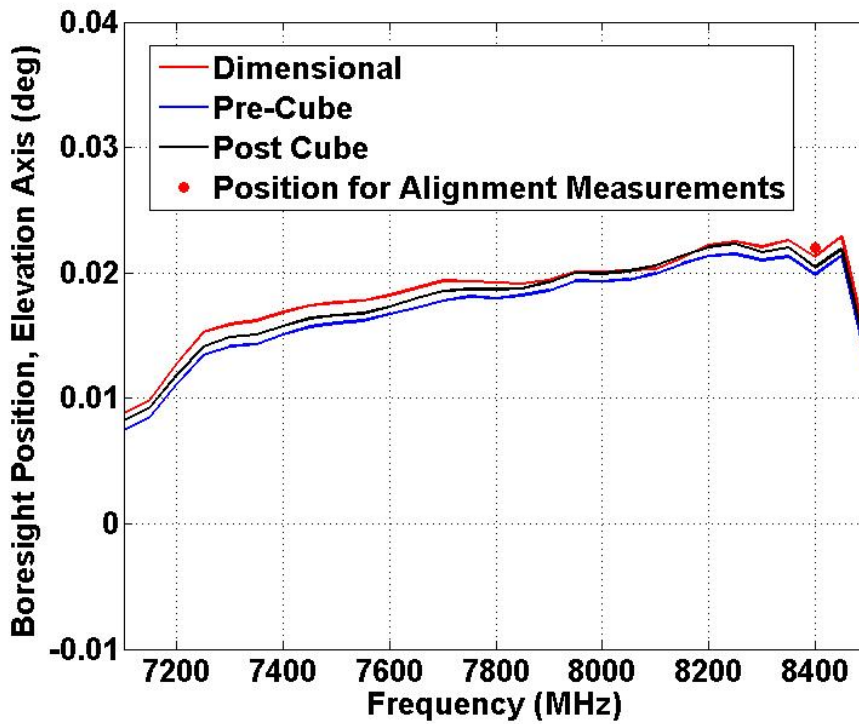


Figure 24b: HGA Boresight Position, Elevation Axis versus Frequency